DMD Fast Forward. Published on October 7, 2011 as doi:10.1124/dmd.111.041954
This article has not been copyedited and formatted. The final version may differ from this version.

DMD # 41954

Prediction of human metabolism of FK3453 by aldehyde oxidase using chimeric mice transplanted with human or rat hepatocytes

Seigo Sanoh, Kazuyoshi Nozaki, Hidetsugu Murai, Shigeyuki Terashita, Toshio Teramura, and Shigeru Ohta

Graduate School of Biomedical Sciences, Hiroshima University, Hiroshima, Japan (S.S., and S.O.); and Analysis & Pharmacokinetics Research Labs., Astellas Pharma Inc., Ibaraki, Japan (K.N., H.M., S.T., and T.T.)

DMD Fast Forward. Published on October 7, 2011 as DOI: 10.1124/dmd.111.041954
This article has not been copyedited and formatted. The final version may differ from this version.

a) Running title: Metabolism by aldehyde oxidase in human liver chimeric mice

b) Corresponding author: Seigo Sanoh

Graduate School of Biomedical Sciences, Hiroshima University, Kasumi 1-2-3, Minami-ku, Hiroshima 734-8553 Japan

Telephone number +81-82-257-5327

Fax number +81-82-257-5329

E-mail address sanoh@hiroshima-u.ac.jp

c) Number of text pages: 37

Number of tables: 3

Number of figures: 5

Number of references: 36

Number of words in abstract: 212

Number of words in introduction: 512

Number of words in discussion: 1165

d) Abbreviations

CYP, cytochrome P450; AO, aldehyde oxidase; PK, pharmacokinetics; h-PXB mice, chimric mice with humanized liver; r-PXB mice, chimeric mice transplanted with rat

hepatocytes; UGT, UDP-glucuronosyltransferase; SULT, sulfotransferase; A-M, AO-generated metabolite; $uPA^{+/+}$, urokinase-type plasminogen activator; SCID, severe combined immunodeficiency; RI, replacement index; h-hepatocytes, h-PXB mice hepatocytes; r-hepatocytes, r-PXB mice hepatocytes; DMSO, dimethylsulfoxide; PEG400, polyethylene glycol 400; C_{max}, the maximum plasma concentration; t_{max}, the time at which C_{max} was achieved; AUC, the area under the plasma concentration-time curve; CL_t, total clearance; i.v., intravenous administration; CL_{oral}, oral clearance; p.o., oral administration; $t_{1/2,}$ half life; F, the oral bioavailability; $CL_{int,\ in\ vitro}$, in vitro intrinsic clearance; $CL_{int,\ in\ vivo}$, in vivo intrinsic clearance; NCEs, new chemical entities.

DMD Fast Forward. Published on October 7, 2011 as DOI: 10.1124/dmd.111.041954
This article has not been copyedited and formatted. The final version may differ from this version.

Abstract

During drug development, it is important to predict the activities of multiple metabolic enzymes, not only cytochrome P450 (CYP) but also non-CYP enzymes, such as conjugative enzymes and aldehyde oxidase (AO). In this study, we focused on prediction of AO-mediated human metabolism and pharmacokinetics (PK) of FK3453 (Astellas Pharma Inc.), development of which was suspended due to extremely low exposure in human, despite good oral bioavailability in rat and dog. We examined species difference in oxidative metabolism of the aminopyrimidine moiety of FK3453, catalyzed by AO, using human-chimeric mice with humanized liver (h-PXB mice) and rat-chimeric mice (r-PXB mice) transplanted with rat hapatocytes. AO activity of h-PXB mouse hepatocytes was higher than that of r-PXB mouse hepatocytes. Moreover, higher concentrations of human-specific AO-generated FK3453 metabolite A-M were detected in urine and feces after administration of FK3453 to h-PXB mice versus r-PXB mice. The total clearance of h-PXB mice was 2-fold higher than that of r-PXB mice. These results agreed reasonably well with the metabolism and PK profiles of FK3453 in human and rat. Our results indicated that h-PXB mice should be helpful for predicting the metabolic profile of drugs in humans, and the use of both h-PXB and r-PXB mice should be helpful for evaluation of species differences of AO metabolic activity.

Introduction

It is important to predict drug metabolism and pharmacokinetics (PK) in human during the pre-clinical stage of pharmaceutical development, since new drug candidates with diverse chemical structures may be metabolized by not only cytochrome P450 (CYP), but also non-CYP enzymes, such as UDP-glucuronosyltransferase (UGT), sulfotransferase (SULT), aldehyde oxidase (AO), xanthine oxidase (Beedham et al., 1997). In recent years, the drop-out rate during drug development has been decreasing as a result of improved predictability of human drug metabolism and PK parameters (Kola et al., 2004). However, it is still difficult to predict non-CYP metabolism, especially involving AO.

AO is a molybdoflavoprotein (Beedham, 1987, Garattini et al., 2003) that catalyzes the metabolism of not only aldehydes, but also nitrogenous heterocycles; it is involved in the oxidative metabolism of drugs such as 6-deoxypenciclovir, 6-mercaptopurine, 5-fluoro-2-pyrimidinone, methotrexate, and zaleplon (Guo et al., 1995, Rashidi et al., 1997, Kawashima et al., 1999, Kitamura et al., 1999, Lake et al., 2002, Rashidi et al.,2007). Moreover, in the presence of its electron donor, AO can mediate the reduction of a variety of compounds, such as sulfoxides, *N*-oxides, and nitrosamines (Kitamura et al., 2006). AO activity shows significant species differences due to the presence of multiple genes coding for AO isoforms (Garattini et al., 2011).

FK3453 [6-(2-amino-4-phenylpyrimidine-5-yl)-2-isopropylpyridazin-3(2H)-one] is a drug

developed as a novel adenosine A1/2 dual inhibitor for the treatment of Parkinson's disease by Astellas Pharma Inc. (Akabane et al, 2011), but its development was suspended due to extremely low systemic exposure in a clinical study, despite encouraging results in animal experiments. FK3453 is metabolized by AO, and the oxidative metabolite of the aminopyrimidine moiety was identified as the major metabolite in plasma after dosing of FK3453 in human. Akabane et al. (2011) suggested that the formation of the AO-generated metabolite (A-M), [6-(2-amino-6-oxo-4-phenyl-1,6-dihydropyrimidin-5-yl)-2-isopropyl pyridazin-3(2H)-one], accounted for the poor oral bioavailability in humans. Species differences of metabolism and disposition had resulted in the failure to predict the poor results in human.

Chimeric mice with humanized liver, generated using urokinase-type plasminogen activator ($uPA^{+/+}$)/severe combined immunodeficiency (SCID) mice repopulated with human hepatocytes (h-PXB mice; Phonixbio, Co., Ltd.) have been reported (Tateno et al., 2004). The expression levels and metabolic activities of CYP and non-CYP enzymes in liver of h-PXB mice were similar to those in human (Katoh et al., 2004, 2005), and human-specific metabolites were detected in h-PXB mice (Inoue et al., 2009, Yamazaki et al, 2010, Kamimura et al., 2010, Serres et al., 2011). Thus, h-PXB mice could be a good in vivo model for predicting drug metabolism in humans. In addition to h-PXB mice, rat-chimeric mice (r-PXB mice) containing high levels of rat hepatocytes have been used to compare

DMD Fast Forward. Published on October 7, 2011 as DOI: 10.1124/dmd.111.041954
This article has not been copyedited and formatted. The final version may differ from this version.

metabolism between rats and humans (Tateno et al., 2004, Emoto et al., 2005). Yamazaki et al. (2010) reported that human-specific metabolites of the pyrazolopyrimidine moiety could be distinguished from rat metabolites by using h-PXB mice and r-PXB mice.

In this study, we performed both in vitro and in vivo investigations using h-PXB mice and r-PXB mice to evaluate the usefulness of these models for predicting human metabolism and PK of FK3453.

Materials and Methods

Chemicals

FK3453 and its metabolite, A-M, were supplied by Astellas Pharma Inc. All other reagents and solvents were commercial products of the highest available grade or analytical grade.

Animals

H-PXB mice and r-PXB mice, in which the endogenous hepatocytes had been replaced with human hepatocytes and rat hepatocytes, respectively, were prepared by PhoenixBio Co. Ltd. (Hiroshima, Japan) according to the method described previously (Tateno et al., 2004, Emoto et al., 2005). Hepatocytes of a human donor (African American male, 5 years old) for transplantion to prepare h-PXB mice were obtained from BD Biosciences (San Jose, CA). Rat hepatocytes for transplantion to prepare r-PXB mice were isolated from liver of Sprague-Dawley (SD) rats (4 weeks of age, male).

The extent of replacement of host hepatocytes with human hepatocytes or rat hepatocytes, calculated as replacement index (RI), was determined by measurement of the concentration of human or rat albumin in blood collected from the tail vein of each PXB mouse. The RI was estimated by the correlation curve between the human albumin levels in mouse blood and determined by using human-specific cytokeratin 8/18-immunostained liver sections (Tateno et al, 2004). Average RI values of h-PXB mice and r-PXB mice used in this study were 83% and

nearly 100%, respectively, as estimated from the corresponding albumin level in blood.

The h-PXB mice and r-PXB mice were housed in a temperature and humidity-controlled environment under a 12 hr/12 hr light/dark cycle with free access to tap water and diet (h-PXB mice, CRF1 diets containing vitamin C; r-PXB mice, normal diet).

All animal studies were approved by the institutional animal ethics committee and conducted in accordance with the regulations on the use of living modified organisms at each facility.

Isolation and purification of hepatocytes from h-PXB mice and r-PXB mice

Hepatocytes was isolated from h-PXB mice and r-PXB mice (13 and 12 weeks of age, respectively) using in situ collagenase perfusion (Yamasaki et al., 2010). h-PXB mice hepatocytes (h-hepatocytes) originally contained about 13% of mouse hepatocytes, although r-PXB mice hepatocytes (r-hepatocytes) were almost free of mouse hepatocytes. Therefore, we employed h-hepatocytes purified from chimeric hepatocytes of h-PXB mice by the use of 66Z rat IgG and magnetic beads bearing anti-rat IgG antibodies. The magnetic removal of mouse hepatocytes reduced the level of mouse hepatocytes to approximately 2%; in this study, purity of human hepatocytes values of h-hepatocytes ranged from 97.4% to 98.3%. Cell viability of hepatocytes used in experiments was more than 78-91% (trypan blue exclusion test).

In vitro metabolic study using h-hepatocytes and r-hepatocytes

Hepatocyte suspension ($1x10^6$ cells /mL) was incubated in Krebs-Henseleit buffer without serum after treatment with 10 μM FK3453 at 37ºC under an atmosphere of 5% CO_2 /95% O_2. The final concentration of acetonitrile was 0.5% (v/v) in the reaction mixture. The plates (24 wells) were shaken gently with an orbital shaker. The incubation mixtures were collected at 0, 0.25, 0.5, 1, and 2 hr after treatment, and frozen in liquid nitrogen. Samples were thawed for analysis and spiked with 2 volumes of acetonitrile. After centrifugation, aliquots of the supernatant were subjected to LC/MS/MS.

Administration of FK3453

FK3453 solution was administered to PXB mice at a single dose of 3 mg/kg. FK3453 was formulated in 10% DMSO, 10% PEG400 with an equivalent amount of hydrochloride in saline for intravenous dosing and in 50% PEG400 with an equivalent amount of hydrochloride in saline for oral dosing. Blood samples were collected from the orbital vein of PXB mice during 0 to 6 hr postdose using heparinaized glass. Plasma samples separated after centrifugation were stored at -30ºC.

Urinary and fecal excretion

Pooled urine and feces after administration were collected during the period of 0 to 24 hr.

Each metabolic cage was washed with water after collection of urine and feces. Samples of urine and feces were homogenized with 10 volumes of water, and the homogenates were stored at -30ºC.

Plasma protein binding

Plasma protein binding ratio of FK3453 (1 μg/mL) in h-PXB and r-PXB mice was determined by equilibrium dialysis after incubation of each plasma with FK3453.

Determination of metabolite profile

Hepatocyte suspension after 2 hr incubation (150μL), urine (150μL), 10% of fecal homogenate (200μL), and pooled plasma (50μL) were mixed with equivalent volumes of acetonitrile and centrifuged at 14000 g for 5 min. The supernatants were subjected to LC/MS/MS.

Aliquots of 5 μL were introduced into a Acquity UPLC® system (Waters, Milford, MA) with a Waters Acquity BEH C18 column, 1.7 μm, 2.1 x 100 mm. The mobile phase consisted of 5 mM ammonium formic acid containing 5% acetonitrile (solvent A) and acetonitrile (solvent B). The flow rate was 0.2 mL/min. The starting condition for the gradient was 100:0 (A:B) until 2.5 min, then the mobile phase composition was changed linearly to 65:35 (A:B) from 2.5 min to 25 min, and 10:90 (A:B) was maintained until 27 min. The gradient was returned

to 100:0 (A:B) from 27 min to 27.01 min for re-equilibration. UV detection at 254 nm was employed. The retention times of FK3453 and A-M were 19.9 min and 16.3 min, respectively. The MS/MS experiments were performed on a Thermo LTQ Orbitrap Velos (Thermo Fisher Scientific, Waltham, MA).

The parameters for the ESI source were as follows: capillary temperature 330ºC; spray voltage 4.5 kV (positive ion mode) or 4.0 kV (negative ion mode); sheath gas flow rate 40 arbitrary unit (nitrogen gas); auxiliary gas flow rate 10 (nitrogen gas); The mass spectrometer was operated in both positive and negative ion modes. The ions were monitored from *m/z* 150 to 800. Normalized collision energies for MS2, MS3 and MS4 were set at 35%, 40%, and 30%, respectively.

Quantitation of FK and its metabolite, A-M

Hepatocyte suspension after 2 hr incubation (20μL), urine (20μL), and plasma (15μL) were each mixed with 2 volumes of acetonitrile and internal standard solution (carbamazepine). The supernatants after centrifugation at 14000 g for 5 min were injected into the LC/MS/MS. 10% of fecal homogenates (200μL) were extracted with 5mL of t-butylmethylether and internal standard solution (carbamazepine). The organic layer (4mL) were evaporated to dryness, the residues were dissolved in aqueous acetonitrile (200μL). Aliquots of 10 μL were applied to an Inertsil ODS-3 (3 μm, 50 x 2.1 mm) column on a HP-1100 series HPLC

instrument (Agilent Technologies, Santa Clara, CA) at 40ºC. The mobile phase was composed of 10 mM ammonium acetate (solvent A) and acetonitrile (solvent B), and the flow rate was 0.2 mL/min. The isocratic condition for HPLC was 70:30 (A:B). The MS/MS experiments were conducted by using an API2000 LC/MS/MS system (Applied Biosystems, Foster, CA). Mass numbers of molecular and product ions used for identification of FK3453 and A-M were as follows: FK3453 *m/z*=308.1 $[M+H]^+$ to 265.9, A-M *m/z*=324.1 $[M+H]^+$ to 281.8. The retention times of FK and A-M were 3.6 and 1.6 min, respectively.

Determination of PK parameters

Pharmacokinetic parameters were determined by non-compartmental methods using the concentration-time curve profile. The maximum plasma concentration (C_{max}) and the time at which the maximum concentration was achieved (t_{max}), which were determined from actual values. The area under the plasma concentration-time curve (AUC) was calculated from the time course using trapezoidal extrapolation from the last quantifiable time to infinity. The total clearance (CL_t) after intravenous administration (i.v.) and the oral clearance (CL_{oral}) after oral administration (p.o.) were calculated as Dose/AUC_{iv} and Dose/AUC_{po}, respectively. The terminal elimination half-life ($t_{1/2}$) was estimated as ln2/slope, where the slope is that of the plot of the terminal elimination phase on a logarithmic scale. The oral bioavailability (F) was calculated as AUC_{po}/AUC_{iv}.

DMD Fast Forward. Published on October 7, 2011 as DOI: 10.1124/dmd.111.041954
This article has not been copyedited and formatted. The final version may differ from this version.

Calculation of in vitro intrinsic clearance ($CL_{int, in\ vitro}$)

In vitro intrinsic clearances ($CL_{int, in\ vitro}$) were calculated from the time course of disappearance of unchanged compound after incubation with hepatocytes of h-PXB mice and r-PXB mice. The disappearance rate constant of unchanged drug was calculated from each plot fitted to the first-order elimination rate constant for FK3453.

DMD Fast Forward. Published on October 7, 2011 as DOI: 10.1124/dmd.111.041954
This article has not been copyedited and formatted. The final version may differ from this version.

Results

In vitro metabolic study using fresh hepatocytes isolated from h-PXB and r-PXB mice

Chemical structures of FK3453 and its AO-generated metabolite, A-M, are shown in Fig.1. AO was confirmed to be responsible for A-M formation by means of an in vitro experiment using AO inhibitor with liver cytosol (Akabane et al, 2011). Fig. 2 shows depletion profiles of FK3453 up to 2 hr during incubation with fresh hepatocytes isolated from PXB mice. Loss of FK3453 was observed during incubation with both h-hepatocytes and r-hepatocytes. In vitro intrinsic clearances (CL_{int}) in h-hepatocytes and r-hepatocytes were 10 and 5 μL/min/10^6 cells, respectively, calculated from the first-order elimination rate constants of FK3453 on a logarithmic scale. Formation of A-M increased, concomitantly with the disappearance of FK3453. The formation of A-M after 2 hr incubation with h-hepatocytes was 15-fold higher than in the case of r-hepatocytes (Table 1). Although A-M was the predominant metabolite with human hepatocytes, not only A-M but also several other peaks were detected with both h-hepatocytes and r-hepatocytes. However, few metabolites were detected with h-hepatocytes, whereas many metabolites besides A-M were found with r-hepatocytes (Fig. 3A, B, Table 1).

Metabolites of FK3453 in urine, feces, and plasma of h-PXB and r-PXB mice

Plasma, urine and feces pooled during 24 hr after i.v./p.o. administration of FK3453 were collected. Excretions of FK3453 in urine and feces amounted to the range from 0.1% to 1.1% of

DMD Fast Forward. Published on October 7, 2011 as DOI: 10.1124/dmd.111.041954
This article has not been copyedited and formatted. The final version may differ from this version.

the dose in h-PXB mice and r-PXB mice, which were very low. The metabolites found in plasma were approximately similar to those of urine, and feces in both h-PXB mice and r-PXB mice except for M11. In contrast, A-M was the predominant metabolite in urine and feces of h-PXB mice, whereas urinary and fecal excretion of A-M was less in r-PXB mice. Other metabolites besides A-M were found in both h-PXB mice and r-PXB mice. In particular, M6, M9, M10, and M12 were specifically detected in plasma, urine, and feces of r-PXB mice but not h-PXB mice (Fig. 4 A,B,C,D,Table 1).

PK profile of FK3453 in h-PXB mice and r-PXB mice

Plasma concentrations and PK parameters after i.v./p.o. administration of FK3453 at 3 mg/kg to h-PXB mice and r-PXB mice are shown in Fig. 5 and Table 2. The values of CL_t after i.v. administration in h-PXB mice and r-PXB mice were 70.7 and 34.0 mL/min/kg, respectively. On other hand, the values of CLoral after p.o. administration were 234.2 and 61.6 mL/min/kg, respectively. Elimination was faster and systemic exposure to FK3453 was lower in h-PXB mice, compared with r-PXB mice. Furthermore, bioavailability of FK3453 after oral dosing in h-PXB mice was lower than that in r-PXB mice.

The value of CL_{oral} calculated from phase I clinical trial data at 10 mg p.o. in human was even higher than that in h-PXB mice. In contrast, the values of CL_{oral} measured in r-PXB mice were approximately similar to those in rats dosed at 3.2 mg/kg (Akabane et al, 2011).

DMD Fast Forward. Published on October 7, 2011 as DOI: 10.1124/dmd.111.041954
This article has not been copyedited and formatted. The final version may differ from this version.

Plasma protein binding of FK3453

Plasma binding ratios of FK3453 in h-PXB mice and r-PXB mice were 79.5% and 76.7%, respectively (Table 3). These values were similar to those evaluated in human and rat. The level of human albumin in plasma was 9.9 mg/mL in h-PXB mice, and that of rat albumin was 17.1 mg/mL in r-PXB mice (data not shown).

DMD Fast Forward. Published on October 7, 2011 as DOI: 10.1124/dmd.111.041954
This article has not been copyedited and formatted. The final version may differ from this version.

Discussion

Prediction of the metabolism and PK of new chemical entities (NCEs) in human is important in the early pre-clinical stage of pharmaceutical development. The number of NCEs metabolized by AO also seems to be increasing (Pryde et al., 2010), and this is important because AO activity shows species differences (Grattini et al., 2011). For example, zaleplon is metabolized by AO to 5-oxo-zaleplon, the major circulating metabolite in human, whereas deacetyl-zaleplon, a CYP3A metabolite, is the major metabolite in rats, mice, and dogs (Kawashima et al., 1999). Furthermore, human-specific AO metabolites of SGX523 were reported to cause acute renal failure in human (Diamond et al, 2010). Zhang et al. (2011) reported that the clinical development of RO1, containing a pyridopyrimidine moiety, as a p38 kinase inhibitor candidate was terminated because of its rapid clearance by AO in human. In addition, famciclovir, methotrexate, zebularine, zoniporide and other similar compounds are AO substrates (Rashidi et al., 1997, Kitamura et al., 1999, Klecker et al., 2006, Dalvie et al., 2010). Generally, AO activity seems to be high in monkey and human, but low in rat and absent in dog. Zientek et al. (2010) established a method for clearance prediction using human liver cytosol and S9 fraction, and obtained a good in vitro-in vivo correlation of intrinsic clearance (CL_{int}) for compounds metabolized by AO. However, in vitro CL_{int} was lower than in vivo CL_{int}, probably owing to partial inactivation of AO during experimental procedures.

While favorable PK profiles of FK3453 were observed in rats and dogs, systemic exposure of

FK3453 in humans turned out to be very low. This finding was considered to be due to high AO activity in human, and indeed, a high plasma concentration of A-M, the AO-catalyzed metabolite of FK3453, was detected in human (Akabane et al., 2011). A-M does not show pharmacological activity (data not shown).

Here, we further examined species differences of AO activity towards FK3453 using h-PXB mice and r-PXB mice. The expression and activity of AO in liver of h-PXB mice have been reported (Kitamura et al., 2008). On the other hand, the AO activity of r-PXB mice seems to be low, probably because rat hepatocytes for r-PXB mice were derived from Crj:SD rats, which show lower AO activity than other strains of rats (Moriyasu et al., 2006, Sugihara et al, 2006, Itoh et al, 2007).

The levels of expression CYP and non-CYP enzymes and metabolic activities in fresh h-hepatocytes are similar to those of actual human hepatocytes (Yoshitsugu et al, 2006, Yamasaki et al, 2010).

$CL_{int,\ in\ vitro}$ calculated from the disappearance rate of FK3453 in h-hepatocytes was 2-fold greater than that in r-hepatocytes (Fig. 2), in agreement with the difference of CL_t between h-PXB mice and r-PXB mice. Moreover, A-M was the predominant metabolite when FK3453 was incubated with h-hepatocytes. In contrast, other metabolites were generated instead of lower A-M formation in r-PXB mice (Fig.2, Fig. 3A, B). We confirmed that A-M formation was mediated by AO in h-hepatocytes because this activity was inhibited by an AO inhibitor,

menadione, but not by a CYP inhibitor, 1-aminobenzotriazole (data not shown). This is in agreement with the findings of Akabane et al (2011).

In vivo, unchanged excretion of FK3453 were low in h-PXB mice and r-PXB mice . The metabolites found in plasma were approximately similar to those of urine, and feces in both h-PXB mice and r-PXB mice. A-M was also the major metabolite in urine and feces after i.v./ p.o administration of FK3453 to h-PXB mice. In other hand, many metabolites were detected in plasma, urine and feces of r-PXB mice. In particular, M6, M9, M10, and M12 were specifically detected in r-PXB mice but not h-PXB mice. These metabolites would be formed by CYP, considering each mass.

Futhermore, each in vitro metabolic profile was agreement with in vivo metabolic profiles in h-PXB mice and r-PXB mice, respectively, although M2 observed in urine of h-PXB mice was not detected in h-hepatocytes. In this case, the levels of remaining mouse hepatocytes in liver of h-PXB mice might not influence on in vitro and in vivo metabolic profiles except for M2, because h-hepatocytes almost consisted of human donor hepatocytes.

In the PK study, CL_t or CL_{oral} of h-PXB mice was 2-fold higher than that of r-PXB mice, in agreement with the $CL_{int,\ in\ vitro}$ values. High levels of A-M were observed in urine and feces of h-PXB mice after administration of FK3453 (Fig. 5, Table 1). The CL_{oral} of FK3453 in h-PXB mice was not in agreement with that of human from a phase I clinical trial (Table 2). On the other hand, both CL_t and CL_{oral} of FK3453 in r-PXB mice were approximately similar to

those in actual rats. This discrepancy may be due to significant difference of hepatic blood flow rate between h-PXB mice and human, compared of relationship between r-PXB mice and rats (Davies et al., 1993).

Plasma binding ratios of FK3453 in h-PXB mice and r-PXB mice agreed well with those in actual human and rat determined by equilibrium dialysis (Table 3). This result supports that high levels of human and rat albumins are expressed in blood of the PXB mice (Tateno et al., 2004). Therefore, the difference in A-M formation may be mainly due to species difference in AO, but not species difference of plasma binding.

In this study, we conducted PK study using h-PXB mice which contain about 20% of mice hepatocytes. It is also important to consider the contribution of the metabolism in remaining mice hepatocytes in hepatic of PXB mice. We examined metabolic activity of FK3453 using hepatocytes isolated from SCID mice compared with h-PXB mice. $CL_{int,\ in\ vitro}$ in SCID mouse hepatocytes and h-hapatocytes were 3 and 10 μL/min/10^6 cells, respectively. In both case, total amount of remaining FK3453 and formation of A-M after 2-hr incubation with FK3453 is approximately 100%. These results suggested AO activity of h-hepatocytes were 3-fold higher than that of SCID mouse hepatocytes (data not shown). Remaining m-hepatocytes in h-PXB mice would not affect human PK and metabolism. As a result, it is at least possible to predict from these data that CL of humans is higher than that of rats.

Furthermore, it is known of species differences of AO family that a single AO gene (*AOX1*) is

coding in humans, four gene (*Aox1, Aox3, Aox4, and Aox311*) in mice genomes. Human AOX1 and mice AOX1/AOX3 were known to be metabolized of *N*-heterocyclic molecules in liver. In contrast, AOX4 is highly presented in the Harderian gland and skin of mice, is absent in humans (Garattini et al, 2009, Terao et al, 2009). Evaluation of extra-hepatic metabolism, which shows species differences, may increasingly improve the predictability of AO metabolism in human.

In conclusion, although h-PXB mice have some limitations for prediction of human drug metabolism, our results suggest that the combined use of h-PXB mice and r-PXB mice may be helpful for examining species differences of drug metabolism and for predicting human metabolism during the early stages of drug development.

Acknowledgements

We thank members in PhoenixBio Co. Ltd. for isolation of hepatocytes from PXB mice.

Authorship Contributions

Participated in research design: Sanoh, Murai, Terashita, Teramura, and Ohta

Conducted experiments: Sanoh, and Nozaki

Contributed new reagents or analytic tools: Murai, Terashita, and Teramura

Performed data analisis: Sanoh

Wrote or contributed to the writing of the manuscript: Sanoh, Nozaki, and Ohta

References

Akabane T, Tanaka K, Irie M, Terashita S, and Teramura T (2011) Case report of extensive metabolism by aldehyde oxidase in humans: pharmacokinetics and metabolite profile of FK3453 in rats, dogs, and humans. *Xenobiotica* **41**:372-84.

Beedham C (1987) Molybdenum hydroxylases: biological distribution and substrate-inhibitor specificity. *Prog Med Chem* **24**:85-127.

Beedham C (1997) The role of non-P450 enzymes in drug oxidation. *Pharm World Sci.* **19**:255-63. Review.

Davies B, and Morris T (1993) Physiological parameters in laboratory animals and humans. *Pharm Res*. **10**:1093-1095. Review.

Dalvie D, Zhang C, Chen W, Smolarek T, Obach RS, Loi CM (2010) Cross-species comparison of the metabolism and excretion of zoniporide: contribution of aldehyde oxidase to interspecies differences. *Drug Metab Dispos* **38**:641-54.

Diamond S, Boer J, Maduskuie TP Jr, Falahatpisheh N, Li Y, Yeleswaram S (2010) Species-specific metabolism of SGX523 by aldehyde oxidase and the toxicological implications. *Drug Metab Dispos* **38**:1277-1285.

Emoto K, Tateno C, Hino H, Amano H, Imaoka Y, Asahina K, Asahara T, Yoshizato K (2005) Efficient in vivo xenogeneic retroviral vector-mediated gene transduction into human hepatocytes. *Hum Gene Ther* 16:1168-74.

Garattini E, Mendel R, Romão MJ, Wright R, and Terao M (2003) Mammalian molybdo-flavoenzymes, an expanding family of proteins: structure, genetics, regulation, function and pathophysiology. *Biochem J* **372** :15-32.

Garattini E, Fratelli M, Terao M (2009) The mammalian aldehyde oxidase gene family. *Hum Genomics* **4**:119-30.

Garattini E, and Terao M (2011) Increasing recognition of the importance of aldehyde oxidase in drug development and discovery. *Drug Metab Rev* **43**: 374-86.

Guo X, Lerner-Tung M, Chen HX, Chang CN, Zhu JL, Chang CP, Pizzorno G, Lin TS, and

Cheng YC (1995) 5-Fluoro-2-pyrimidinone, a liver aldehyde oxidase-activated prodrug of 5-fluorouracil. *Biochem Pharmacol* **49**:1111-1116.

Kamimura H, Nakada N, Suzuki K, Mera A, Souda K, Murakami Y, Tanaka K, Iwatsubo T, Kawamura A, and Usui T. (2010) Assessment of chimeric mice with humanized liver as a tool for predicting circulating human metabolites. *Drug Metab Pharmacokinet* **25**:223-235 Review.

Katoh M, Matsui T, Nakajima M, Tateno C, Kataoka M, Soeno Y, Horie T, Iwasaki K, Yoshizato K, and Yokoi T (2004) Expression of human cytochromes P450 in chimeric mice with humanized liver. *Drug Metab Dispos* **32**:1402-1410.

Katoh M, Matsui T, Okumura H, Nakajima M, Nishimura M, Naito S, Tateno C, Yoshizato K, and Yokoi T (2005) Expression of human phase II enzymes in chimeric mice with humanized liver. *Drug Metab Dispos* **33**:1333-1340.

Kawashima K, Hosoi K, Naruke T, Shiba T, Kitamura M, Watabe T (1999) Aldehyde oxidase-dependent marked species difference in hepatic metabolism of the sedative-hypnotic, zaleplon, between monkeys and rats. *Drug Metab Dispos* **27**:422-428.

Kitamura S, Sugihara K, Nakatani K, Ohta S, Ohhara T, Ninomiya S, Green CE, Tyson CA (1999) Variation of hepatic methotrexate 7-hydroxylase activity in animals and humans. *IUBMB Life*. **48**:607-611.

Kitamura S, Sugihara K, and Ohta S (2006) Drug-metabolizing ability of molybdenum hydroxylases. *Drug Metab Pharmacokinet*. **21**:83-98.

Kitamura S, Nitta K, Tayama Y, Tanoue C, Sugihara K, Inoue T, Horie T, Ohta S (2008) Aldehyde oxidase-catalyzed metabolism of N^1-methylnicotinamide in vivo and in vitro in chimeric mice with humanized liver. *Drug Metab Dispos* **36**:1202-5.

Klecker RW, Cysyk RL, Collins JM (2006) Zebularine metabolism by aldehyde oxidase in hepatic cytosol from humans, monkeys, dogs, rats, and mice: influence of sex and inhibitors. *Bioorg Med Chem* **14**:62-66.

Kola I, and Landis J (2004) Can the pharmaceutical industry reduce attrition rates? *Nat Rev Drug Discov* **3**:711-715.

Inoue T, Sugihara K, Ohshita H, Horie T, Kitamura S, and Ohta S (2009) Prediction of human disposition toward S-^{3}H-warfarin using chimeric mice with humanized liver. *Drug Metab Pharmacokinet* **24**:153-60.

Itoh K, Maruyama H, Adachi M, Hoshino K, Watanabe N, Tanaka Y (2007) Lack of dimer formation ability in rat strains with low aldehyde oxidase activity. *Xenobiotica*.**37**:709-16.

Lake BG, Ball SE, Kao J, Renwick AB, Price RJ, Scatina JA. (2002) Metabolism of zaleplon by human liver: evidence for involvement of aldehyde oxidase. *Xenobiotica* **32**:835-847.

Moriyasu A, Sugihara K, Nakatani K, Ohta S, Kitamura S (2006) In vivo-in vitro relationship of methotrexate 7-hydroxylation by aldehyde oxidase in four different strain rats. *Drug Metab Pharmacokinet* **21**:485-491.

Pryde DC, Dalvie D, Hu Q, Jones P, Obach RS, Tran TD (2010) Aldehyde oxidase: an enzyme of emerging importance in drug discovery. *J Med Chem* **53**:8441-8460.

Serres MD, Bowers G, Boyle G, Beaumont C, Castellino S, Sigafoos J, Dave M, Roberts A, Shah V, Olson K, Patel D, Wagner D, Yeager R, Serabjit-Singh C (2011) Evaluation of a

chimeric (uPA$^{+/+}$)/SCID mouse model with a humanized liver for prediction of human metabolism. *Xenobiotica*. **41**:464-475.

Sugihara K, Tayama Y, Shimomiya K, Yoshimoto D, Ohta S, Kitamura S (2006) Estimation of aldehyde oxidase activity in vivo from conversion ratio of *N1*-methylnicotinamide to pyridones, and intraspecies variation of the enzyme activity in rats. *Drug Metab Dispos* **34**:208-12.

Tateno C, Yoshizane Y, Saito N, Kataoka M, Utoh R, Yamasaki C, Tachibana A, Soeno Y, Asahina K, Hino H, Asahara T, Yokoi T, Furukawa T, and Yoshizato K (2004) Near completely humanized liver in mice shows human-type metabolic responses to drugs. Am J Pathol **165**:901-912.

Terao M, Kurosaki M, Barzago MM, Fratelli M, Bagnati R, Bastone A, Giudice C, Scanziani E, Mancuso A, Tiveron C, Garattini E (2009) Role of the molybdoflavoenzyme aldehyde oxidase homolog 2 in the biosynthesis of retinoic acid: generation and characterization of a knockout mouse. *Mol Cell Biol* **29**:357-77.

Rashidi MR, Smith JA, Clarke SE, and Beedham C (1997) In vitro oxidation of famciclovir

and 6-deoxypenciclovir by aldehyde oxidase from human, guinea pig, rabbit, and rat liver. *Drug Metab Dispos.* **25**:805-13.

Rashidi MR, Beedham C, Smith JS, and Davaran S (2007) In vitro study of 6-mercaptopurine oxidation catalysed by aldehyde oxidase and xanthine oxidase. *Drug Metab Pharmacokinet* **22**:299-306.

Yamasaki C, Kataoka M, Kato Y, Kakuni M, Usuda S, Ohzone Y, Matsuda S, Adachi Y, Ninomiya S, Itamoto T, Asahara T, Yoshizato K, and Tateno C (2010) In vitro evaluation of cytochrome P450 and glucuronidation activities in hepatocytes isolated from liver-humanized mice. D*rug Metab Pharmacokinet* **25**:539-50.

Yamazaki H, Kuribayashi S, Inoue T, Tateno C, Nishikura Y, Oofusa K, Harada D, Naito S, Horie T, and Ohta S (2010) Approach for in vivo protein binding of 5-n-butyl-pyrazolo[1,5-a]pyrimidine bioactivated in chimeric mice with humanized liver by two-dimensional electrophoresis with accelerator mass spectrometry. *Chem Res Toxicol*. **23**:152-8.

Yoshitsugu H, Nishimura M, Tateno C, Kataoka M, Takahashi E, Soeno Y,

Yoshizato K, Yokoi T, Naito S (2006) Evaluation of human CYP1A2 and CYP3A4 mRNA expression in hepatocytes from chimeric mice with humanized liver. *Drug Metab Pharmacokinet* **21**:465-474.

Zhang X, Liu HH, Weller P, Zheng M, Tao W, Wang J, Liao G, Monshouwer M, Peltz G (2011) In silico and in vitro pharmacogenetics: aldehyde oxidase rapidly metabolizes a p38 kinase inhibitor. *Pharmacogenomics J*. **11**:15-24.

Zientek M, Jiang Y, Youdim K, and Obach RS (2010) In vitro-in vivo correlation for intrinsic clearance for drugs metabolized by human aldehyde oxidase. *Drug Metab Dispos* **38**:1322-1327

Footnotes

This research was supported by a Grant-in-Aid for Young Scientists (B) from Japan Society for the Promotion of Science [Grant 22790109].

Figure titles and legends

Fig. 1 Chemical structures of FK3453 and its AO metabolite (A-M)

Fig. 2 Time courses of FK3453 (closed square) and A-M (closed triangle) during 2 hrs incubation with h-hepatocytes and r-hepatocytes isolated from h-PXB and r-PXB mice, respectively.

FK3453 (10 μM) was incubated for 2 hrs with h-hepatocytes (left figure) and r-hepatocytes (right figure) at $1x10^6$ cells/mL. Each point and bar represents the mean±S.D. (n=3)

Fig. 3 UV chromatograms of metabolites after incubation of FK3453 with h-hepatocytes (A) and r-hepatocytes (B).

Pooled samples (n=3) of blank, 0 hr, and 2 hr after incubation with h-hepatocytes were chromatographed with detection at 254 nm. Solid arrows indicate metabolites detected by UV and MS. Dotted arrows show metabolites detected by only MS.

Fig.4 UV chromatograms of FK3453 metabolites from urine (A,C) and feces (B,D) of h-PXB mice (A,B) and r-PXB mice (C,D).

Pooled 24-hr samples (n=3) of blank, and after i.v., and p.o. administration to h-PXB mice and r-PXB mice (n=3) were chromatographed with detection at 254 nm. Solid arrows indicate

metabolites detected by UV and MS. Dotted arrows show metabolites detected by only MS.

Fig. 5 Plasma concentration-time curves of FK3453 and A-M in h-PXB mice and r-PXB mice.

Data are mean±S.D. (n=3~4)

Table 1 In vitro and in vivo (i.v./p.o.)comparison of metabolic profiles of FK3453 in h-PXB mice and r-PXB mice

	Retention time (min)	Mass	h-PXB mice				r-PXB mice			
			in vitro	*in vivo*			*in vitro*	*in vivo*		
			Hepatocytes	Plasma	Urine	Feces	Hepatocytes	Plasma	Urine	Feces
FK3453	**20.0**	**M**	27.5%[(a)]	+	0.1% [(b)]	0.1% [(b)]	58.4%[(a)]	+	0.1%[(b)]	1.1% [(b)]
A-M	**16.5**	**M+16**	76.1%[(a)]	+	31.6%[(b)]	21.1%[(b)]	5.1% [(a)]	+	6.5%[(b)]	32.3%[(b)]
M1	**10.0**	**M+192**	+	+	+	−	+	+	+	−
M2	**10.5**	**M+30**	−	−	+	−	+	+	+	+
M3	**11.8**	**M-42**	+	+	+	−	+	+	+	+
M4	**12.4**	**M+32**	+	+	+	+	+	+	+	+
M5	**12.5**	**M+196**	+	+	+	−	−	−	−	−
M6	**13.2**	**M+32**	−	−	−	−	+	+	+	−
M7	**13.5**	**M+14**	+	−	+	−	−	−	−	−
M8	**13.7**	**M+196**	+	+	+	−	+	+	+	−
M9	**14.8**	**M+16**	−	−	−	−	+	+	+	+
M10	**15.6**	**M+16**	−	−	−	−	+	−	+	+
M11	**17.2**	**M-2**	+	+	−	−	+	+	−	−
M12	**17.4**	**M+16**	−	−	−	−	+	+	+	−

+; Metabolites detected by UV or MS. −; Not detected, (a); % values of hepatocytes indicate the ratios of remaining FK3453 and formation of A-M after 2-hr incubation with FK3453 (10 μM). (b); % values of urine and feces indicate excretion ratio as % of dose (i.v.)

Table 2 Comparison of PK parameters of FK3453 among PXB mice, human, and rat.

Species	Dose	i.v.		p.o.			
		$t_{1/2}$	CL_t	C_{max}	AUC	CL_{oral}	F
		hr	mL/min/kg	ng/mL	ng·hr/mL	mL/min/kg	%
h-PXB mice	3.0 mg/kg	0.7	70.7	252.9	213.5	234.2	29.4
Human[(a)]	10 mg/person	No data		1.50	2.19	1087.2	No data
r-PXB mice	3.0 mg/kg	0.8	34.0	855.6	811.4	61.6	52.6
Rat[(b)]	3.2 mg/kg	0.4	10.8	544.0	1789.4	29.8	34.6

(a), (b) PK parameters of human and rat from the literature (Akabane et al, 2011).

Table 3 Summary of plasma protein binding in PXB mice, human, and rat

Species	h-PXB mice	Human[(a)]	r-PXB mice	Rat[(b)]
Protein binding (%)	**79.5 ± 2.1**	**77.2**	**76.7 ± 0.9**	**75.4**

Data are mean ± S.D. of n=3

(a), (b) Protein binding of human and rat from the literature (Akabane et al, 2011)

Fig.1

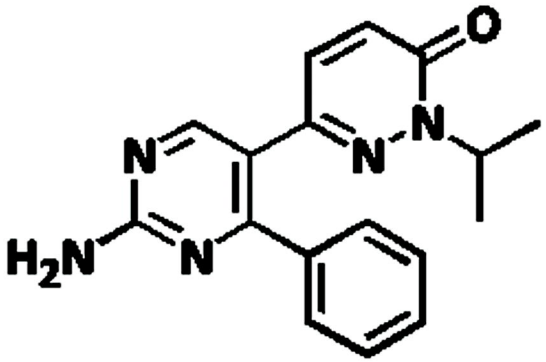

FK3453

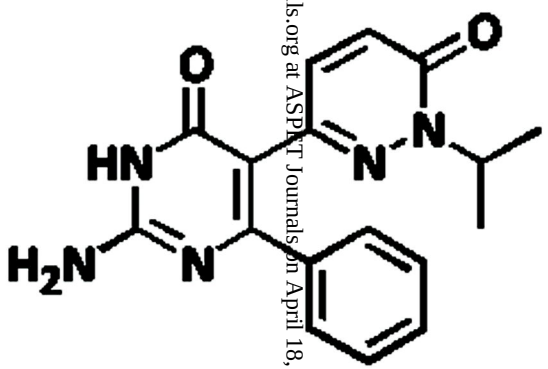

Aldehyde oxidase metabolite (A-M)

Fig.2

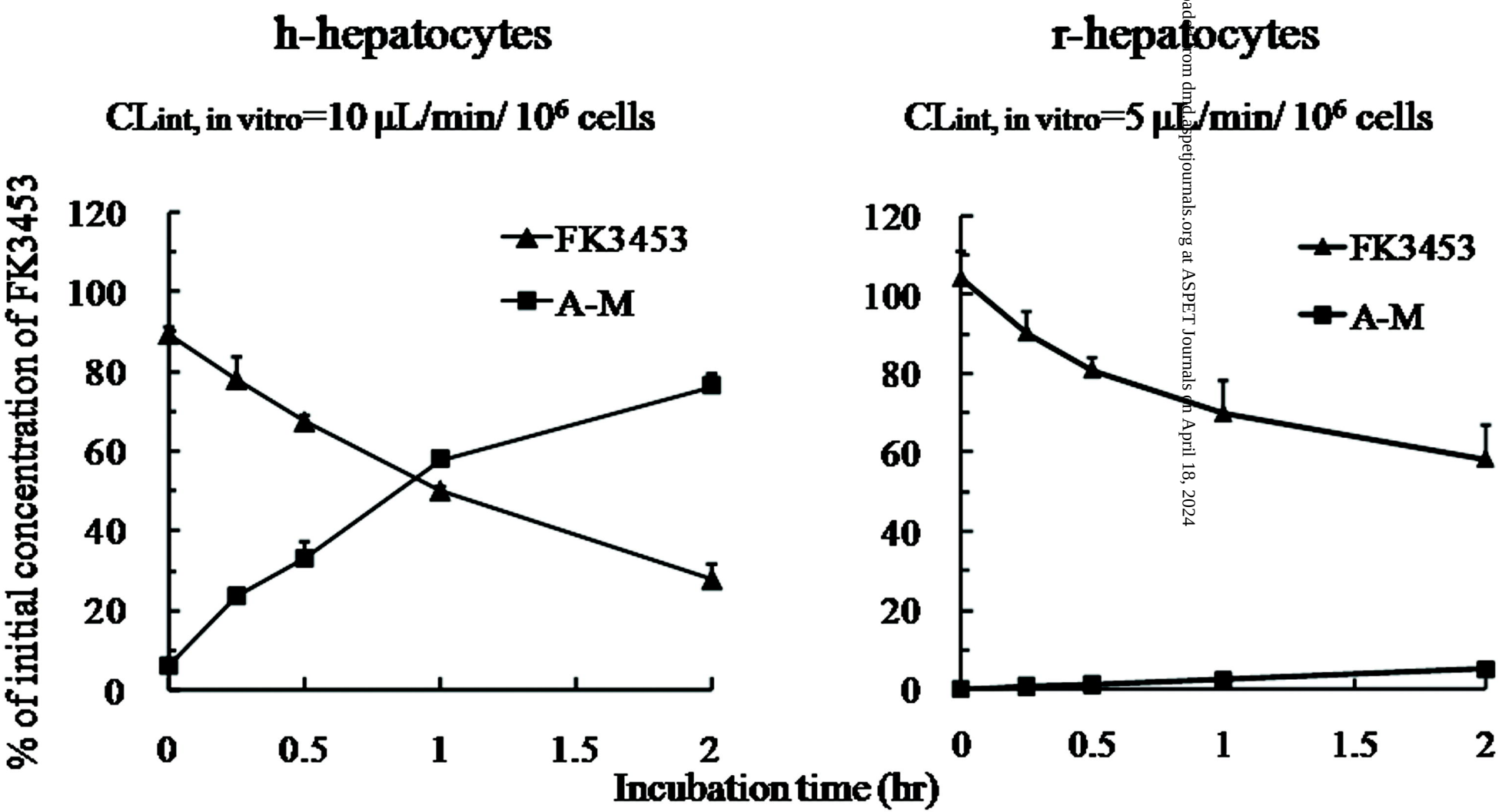

Fig.3 (A)

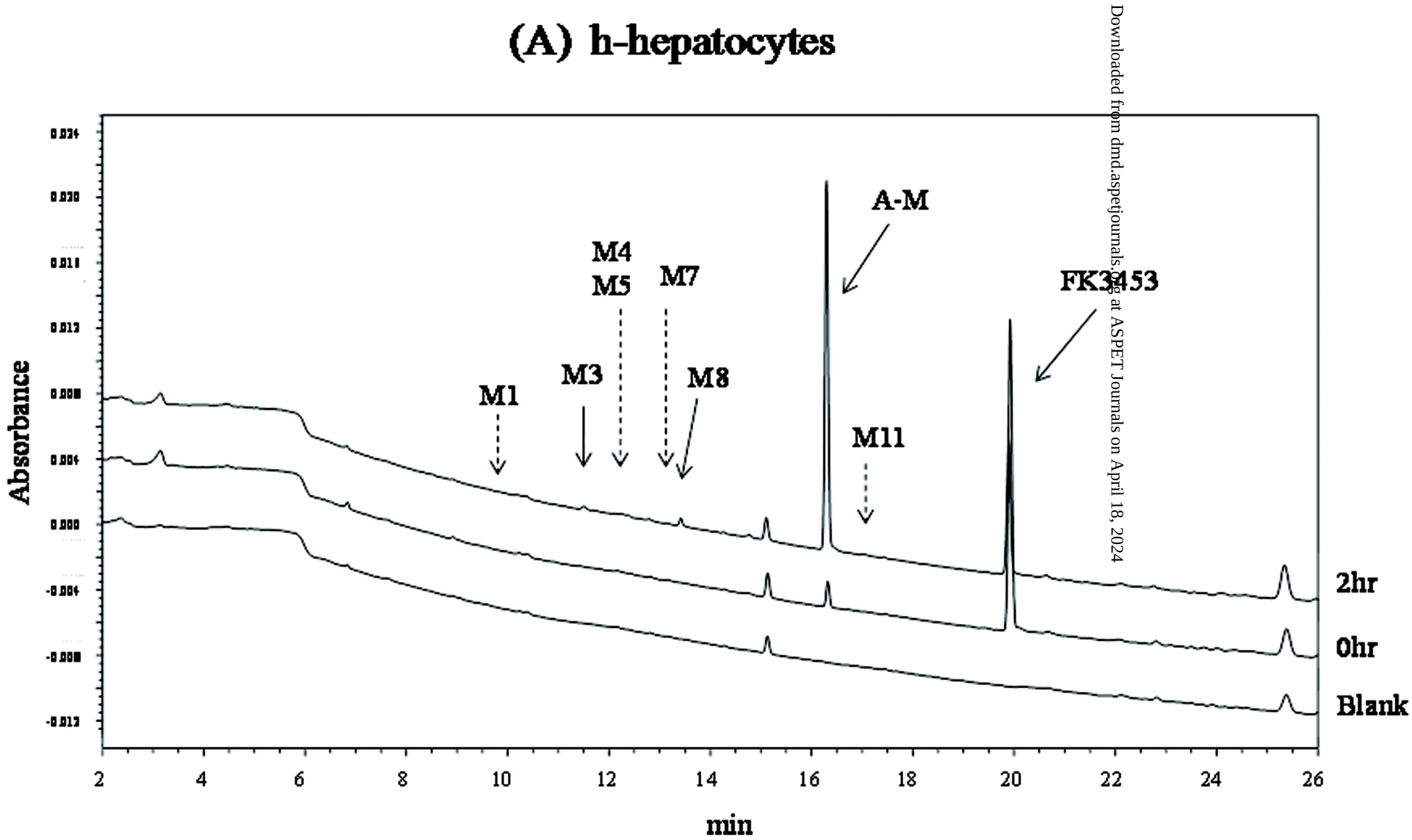

Fig.3 (B)

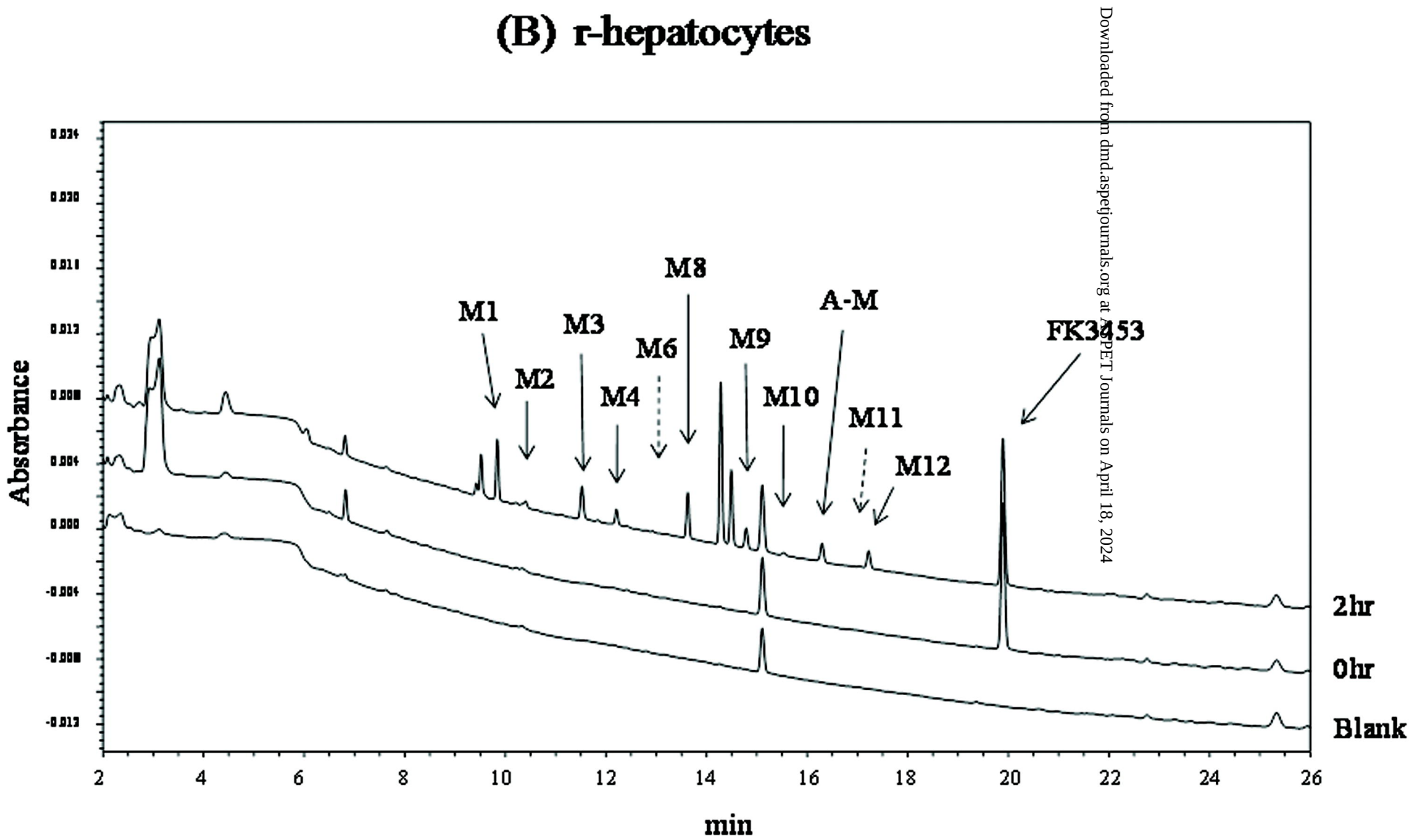

Fig.4 (A)

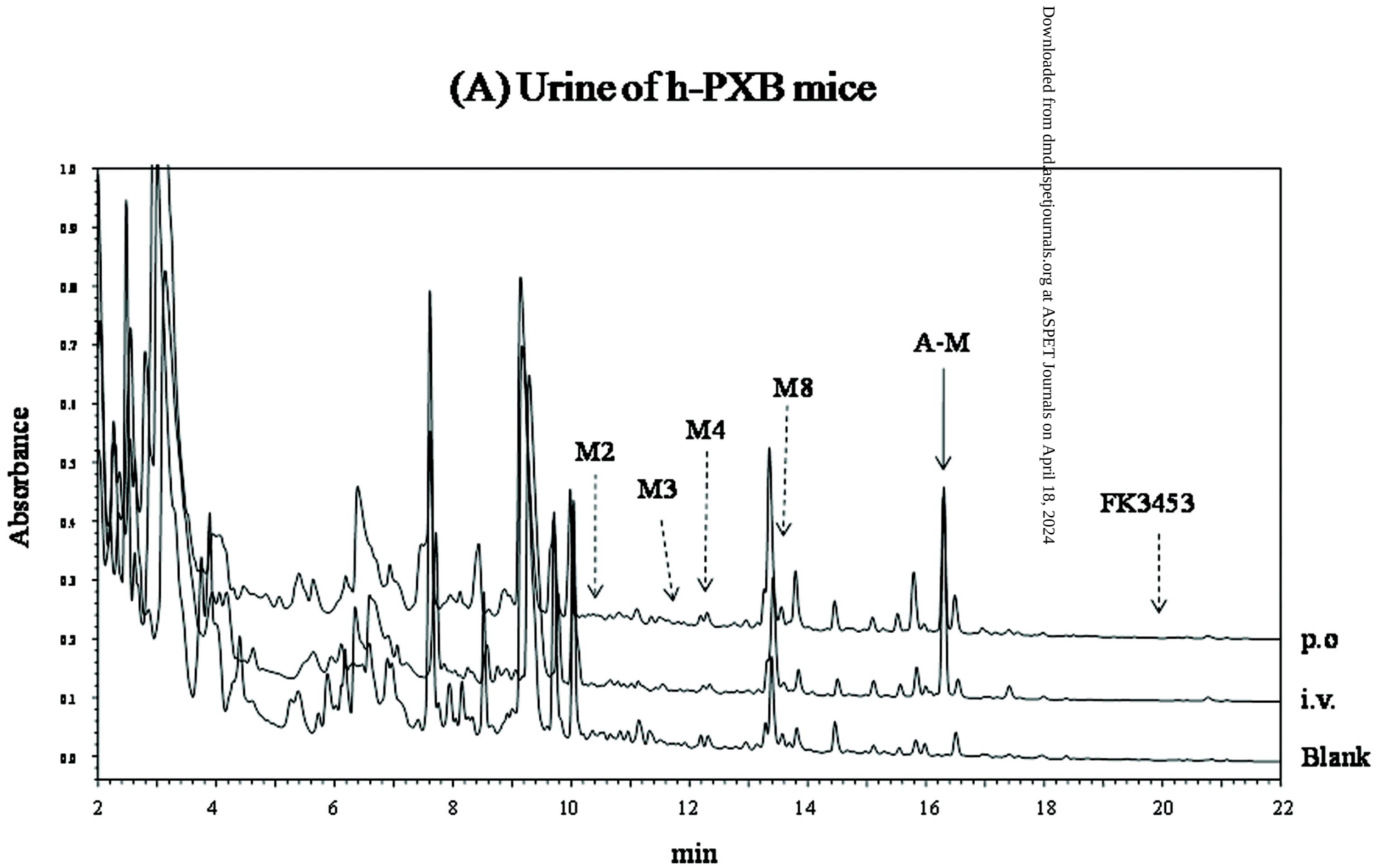

Fig.4 (B)

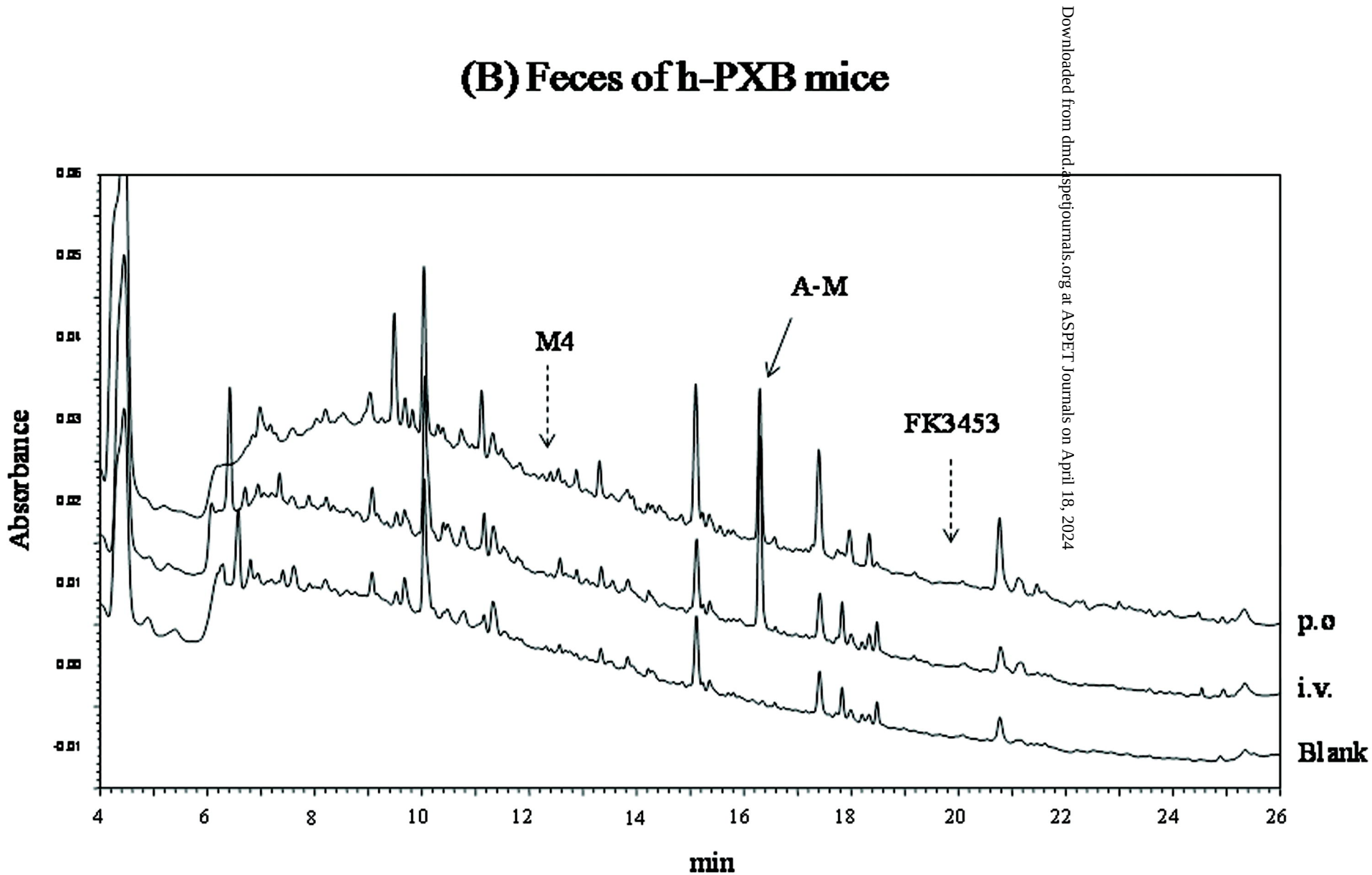

Fig.4 (C)

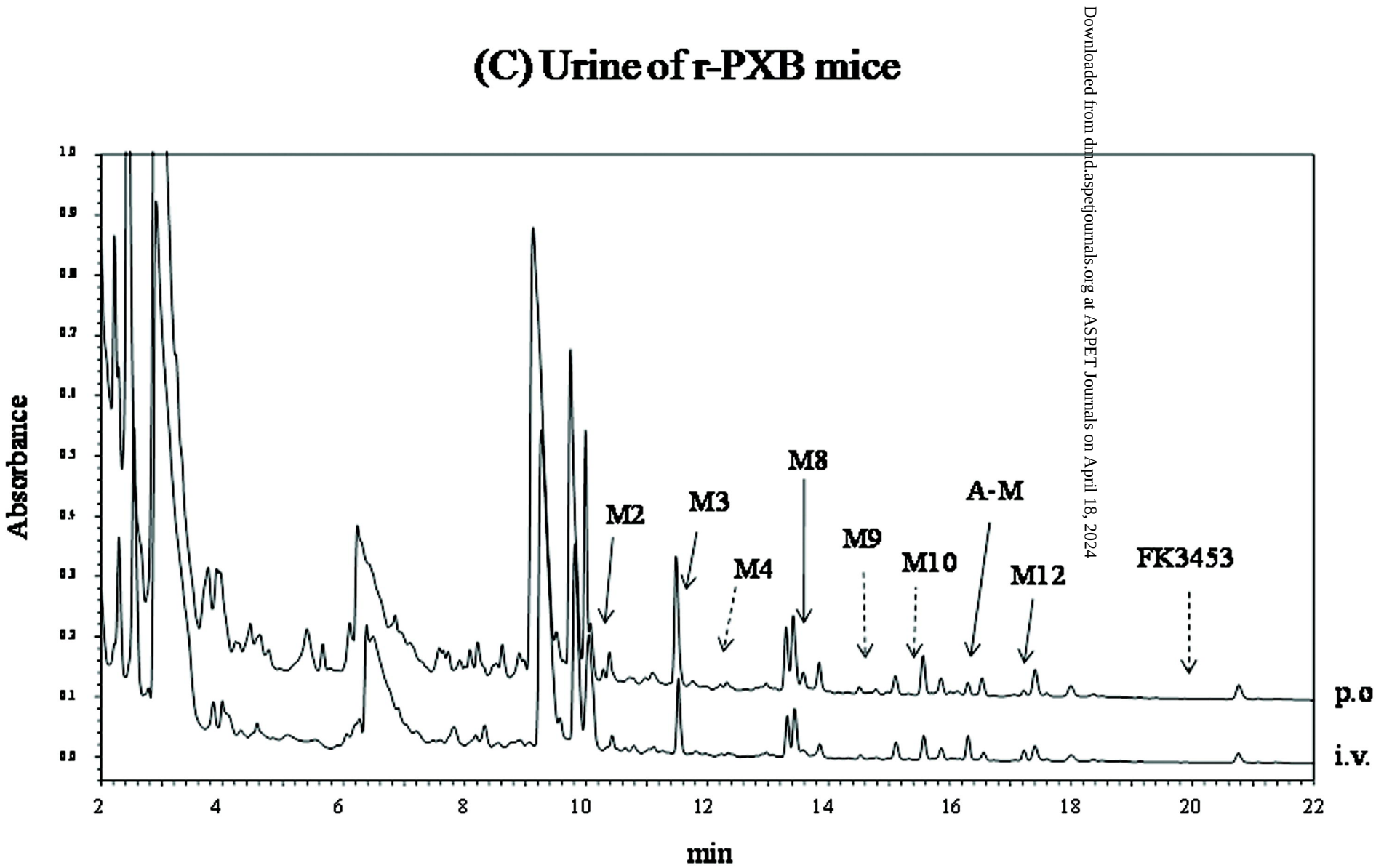

Fig.4 (D)

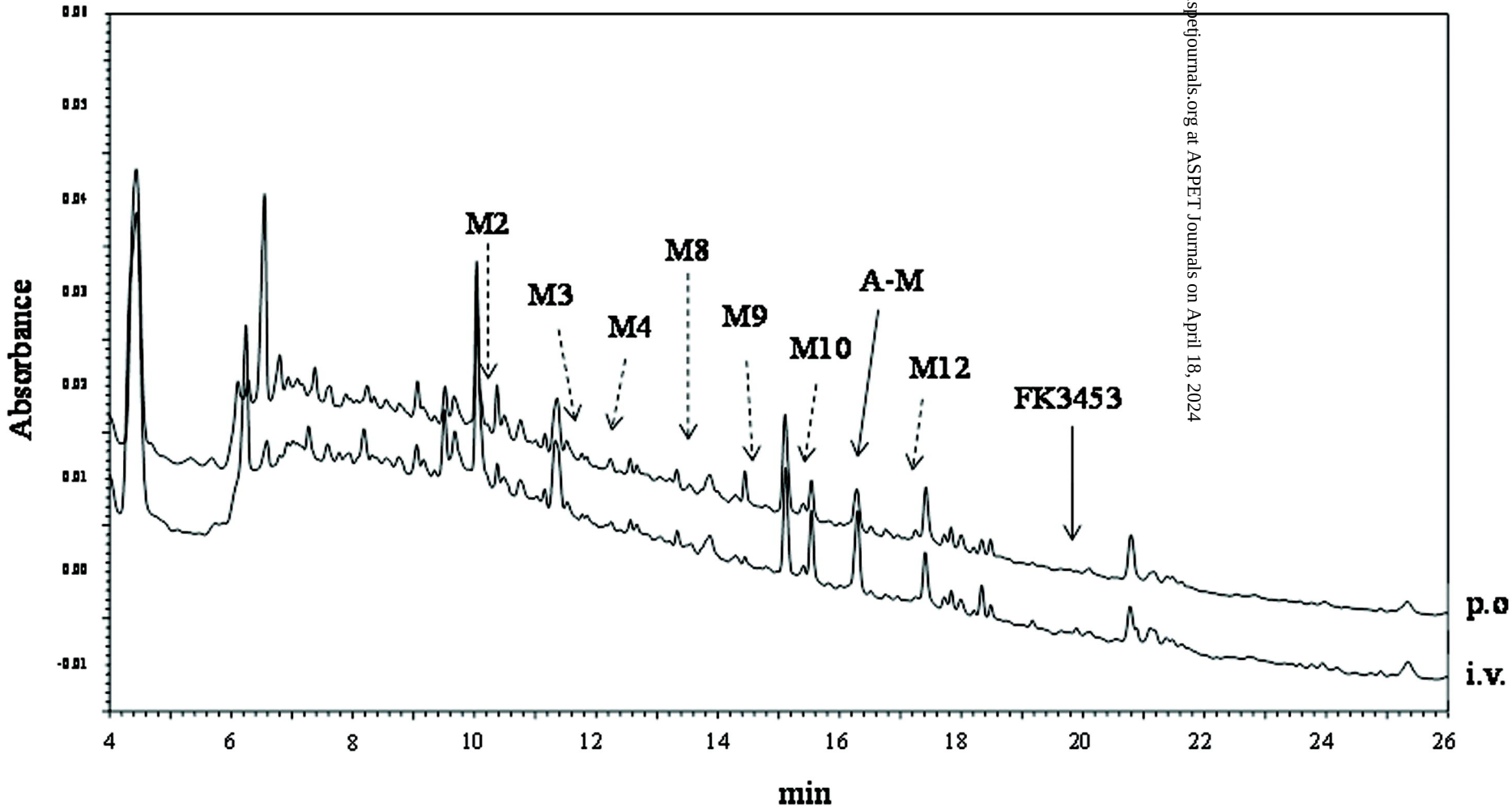

Fig.5